Research Article

A hybrid renewable energy system integrating photovoltaic panels, wind turbine, and battery energies for supplying a grid-connected residential load

Mohammad Jafari[1] · **Zahra Malekjamshidi**[1]

Received: 16 May 2020 / Accepted: 8 October 2020 / Published online: 21 October 2020

Abstract
In this paper, a topology of a multi-input renewable energy system, including a PV system, a wind turbine generator, and a battery for supplying a grid-connected load, is presented. The system utilizes a multi-winding transformer to integrate the renewable energies and transfer it to the load or battery. The PV, wind turbine, and battery are linked to the transformer through a full bridge dc–ac converter and their energy supplied to a grid-connected single-phase inverter and loads. A phase-shift control technique is employed to control the power flow between the sources and loads and the grid. To control the power flow, simple PI controllers have been used. The operation details and control techniques of the system are presented and also validated by using numerical simulations.

Keywords PI control · Multi-port converter · Phase-shift · Multi-winding transformer · PV system · Inverter

1 Introduction

Multi-port converters have been an attractive research topic over the past decade due to their application in the integration of several renewable energy sources into a single power processing unit. Therefore, a large number of multi-port converter topologies have been introduced in the literature so far [1–9]. The proposed topologies can be classified as the topologies operate based on the series or parallel connection of small conversion cells [10], the time-sharing concept [11–13], and magnetic flux additivity [14]. Furthermore, some of them have the property of bidirectional power flow between the connected ports, while others are unidirectional only [15]. Among the proposed topologies, those are based on magnetic-coupling through a multi-winding transformer have attracted more attention due to their excellent features in terms of flexibility, safety, isolation and operational power range. This provides an isolation between the ports and facilitates connecting several sources having substantially different operating voltages thanks to the transformer turns ratio [16]. On the other hand, a simpler power flow control can be achieved by using a phase-shift control technique [17–19]. A complete study on the magnetically coupled multi-port converters have been presented in [16–20]. It should be noted that the system operation and design of multi-winding high-frequency transformer become very complex in the case of large number windings [21–24]. A magnetically coupled converter with two input and one output is presented in [25] where instead of combining input dc sources in electric form, they are combined in magnetic form by adding up the produced magnetic fluxes together using the magnetic core of the multi-winding transformer. The power flow in the proposed converter has been drawn from two different dc sources and delivered to the load individually and simultaneously [16]. The converter is able to accommodate voltage variations

✉ Mohammad Jafari, mohammad.jafari@uts.edu.au | [1]School of Electrical and Data Engineering, University of Technology Sydney, 15 Broadway, Ultimo, NSW 2007, Australia.

SN Applied Sciences (2020) 2:1852 | https://doi.org/10.1007/s42452-020-03654-6

of the sources by using the current-fed H-bridge converters. However, the topology is not able to maintain a bidirectional power flow and the current stress of the switching devices is high [16]. A three-port converter was proposed in [26] to couple a fuel cell and a battery system and the topology was also recommended in [27] for application in an uninterruptible power supply (UPS). Using batteries along the renewable energy sources increases the energy management flexibility [27, 28]. However, many technical points need to be considered when using batteries as energy storage [29]. As another application, a three-port converter is introduced using two current-fed ports to interface several energy storage elements such as batteries and supercapacitors [30]. As a recent application, the magnetically coupled multi-port converter is used in a hybrid energy system for a residential house [17, 19]. The proposed topology enables the system to operate based on the different control techniques and energy management scenarios [16].

The conventional technique of coupling converter ports to the multi-winding transformer is using H-bridge dc–ac converters to generate a high-frequency rectangular waveform from the input dc voltage as discussed in more detail in [16, 31, 32]. The power flow control then can be realized by applying leading or lagging phase shift between the generated waveforms. The topology is suitable for medium-power applications (a few kilowatts) and the main advantages are simultaneous bidirectional power transfer between any input to any output, the possibility of soft-switched operation for all coupled H-bridges, galvanic isolation between the input and outputs, capability of matching different voltage levels using transformer turns ratio and centralized control [16]. However, there are some disadvantages, such as a large number of switching devices, limited soft-switched region when operating with wide input voltage ranges and complexity of transformer design [16, 17]. The problem of soft-switching range in the case of using variable dc sources as the input source can be reduced by applying duty cycle control to the generated waveforms or using current-fed H-bridge converters instead of simple H-bridges [33]. In [34], the authors studied some other bridge converters with possibility of using in the phase-shift converters. To analyze the multi-port phase-shift converters, the multi-port topology can be decomposed into the simple dual active bridge (DAB) converter topologies as is discussed in [6, 16, 35]. The DAB converter was proposed by Kheraluwala and Divan in [36] and more detailed analysis was provided in [37]. The topology has been widely studied in the literature and modified considerably over the last decade. The improvement in the switching conditions of the bridge converter is studied in [38, 39] and the problem of circulating reactive power and possible solutions have been studied [40, 41].

In this paper, a multi-port phase-shift converter topology based on a multi-winding high-frequency transformer for integrating a PV system, a wind turbine generator and a battery is introduced to supply a set of grid-connected domestic loads. The topology has several advantages compared to the other solutions based on the dc and ac bus topologies. It provides galvanic isolation between the ports, a bidirectional power flow by providing a magnetic bus and also an easier way to control the power flow between the ports by using the phase-shift technique. The system is designed to transfer the power from renewable energy sources to the battery, load and grid. However, the power can be supplied from the grid to the battery in the reverse direction when is required which increases the flexibility of the system compared to the other proposed multi-port converter topologies. The system operation principle is discussed in detail and the control technique is also studied. Numerical simulation of the proposed topology and control technique is carried out using PSIM software and the experimental tests are conducted to show the validity of system operation and the proposed control techniques.

2 Operation principle of the proposed converter

The topology of the proposed Multi-port converter is presented in Fig. 1. As illustrated in the figure, the converter topology contains four H-bridge dc-ac converters linked to a multi-winding transformer at one side and to a dc source at the other side. The H-bridge converter in port one is connected to a PV panel as a renewable energy source, port two to a wind turbine generator as the second renewable energy source, port three to a battery as the main energy storage device in the system, and port four to a high-voltage dc bus which is linked to a single-phase inverter and further to the utility grid. In this structure, the transformer core is used as a magnetic coupling bus to transfer the power between the converter ports in a magnetic form [20, 21]. The main advantage of the system is that the ports having different operating voltages are easily matched by transformer turns ratios. They are electrically isolated and their relation is only in the magnetic form [16]. As presented in the figure by arrows on the magnetic core, the power flows mainly from the PV system and wind turbine to the battery and inverter ports; however, a bidirectional power flow also can be realized between the battery and inverter port.

Figure 2 shows the structure of the dc–dc converter with four ports connected to the four winding of the high-frequency transformer. Such a structure is known as a quadruple active bridge (QAB) converter. In this

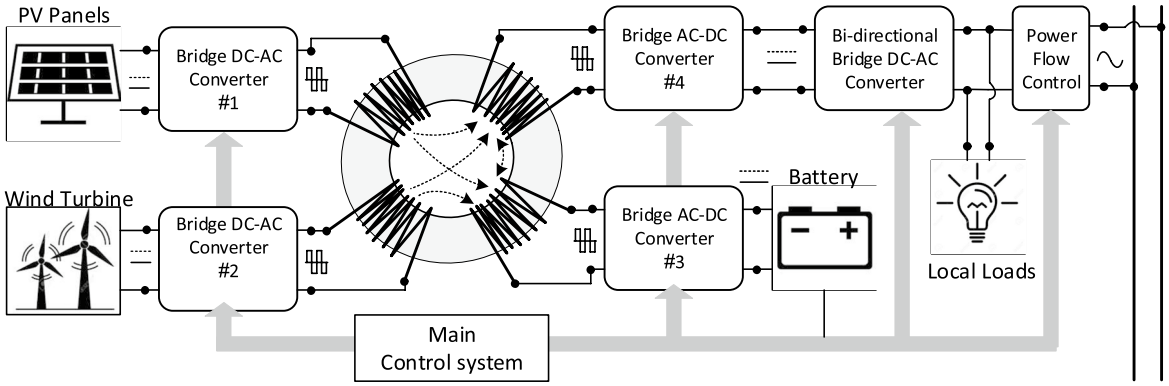

Fig. 1 Topology of the proposed hybrid renewable energy system including the multi-port phase-shift converter and grid-connected inverter

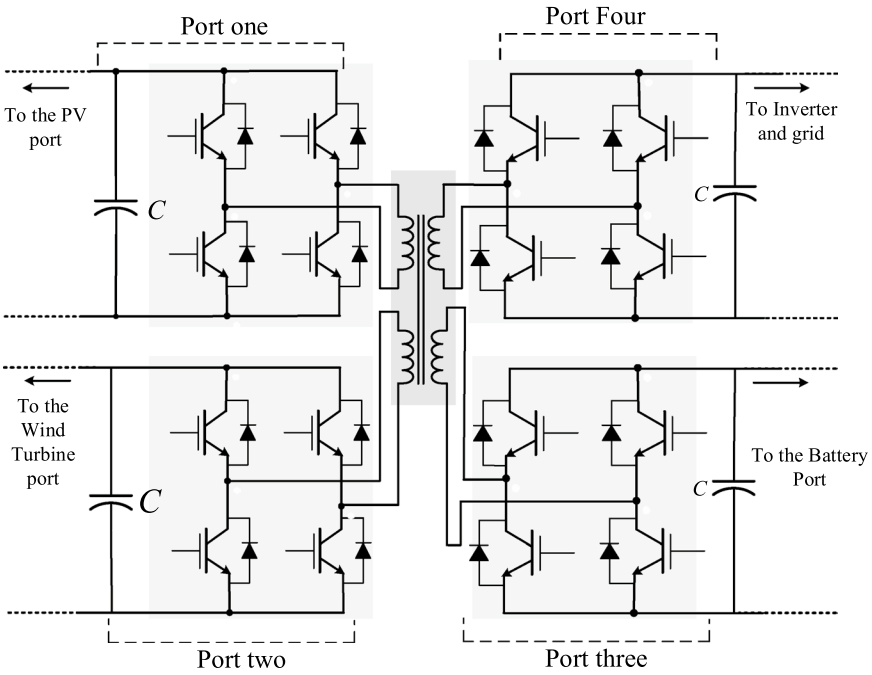

Fig. 2 Structure of QAB converter as a part of the proposed hybrid renewable energy system

structure, the power flow in this system can be controlled by a phase-shift technique as studied in detail in [16, 42]. The H-bridge converter in port four is connected to a high-voltage dc linked as the dc voltage is going to be changed to a single-phase ac voltage by the single-phase inverter (220 Vrms, $f = 50$ Hz). The generated ac voltage then can be supplied to the domestic loads or transferred to the grid as a parallel link. The power also can be supplied by the power to the battery when the inverter is operating as a rectifier if the system is designed to operate as an uninterruptable power supply (UPS). To analyze the power flow in the system, the system can be simplified by using the cantilever model of the multi-winding transformer. The multi-port converter with N-port system can be decomposed into $N(N-1)/2$ two-port converter as illustrated in Fig. 3 [15, 16]. The dc sources and the H-bridge converters are combined and presented as voltage source with a rectangular high-frequency waveform for the sake of simplicity. The structure can be simplified further where all the parameters at the transformer windings in ports 2, 3, and 4 are referred to the winding in port one and the.

Magnetizing inductance is neglected as it has no influence on the power flow. As can be seen, the resultant structure shows that the four-port converter topology can be decomposed in several dual active bridge converter. Therefore, the total power flows from each converter port can be obtained by summation of power flows to each individual port, referring to the simplified model in Fig. 3. The power flow equations in the proposed converter according to Fig. 3 can be written as

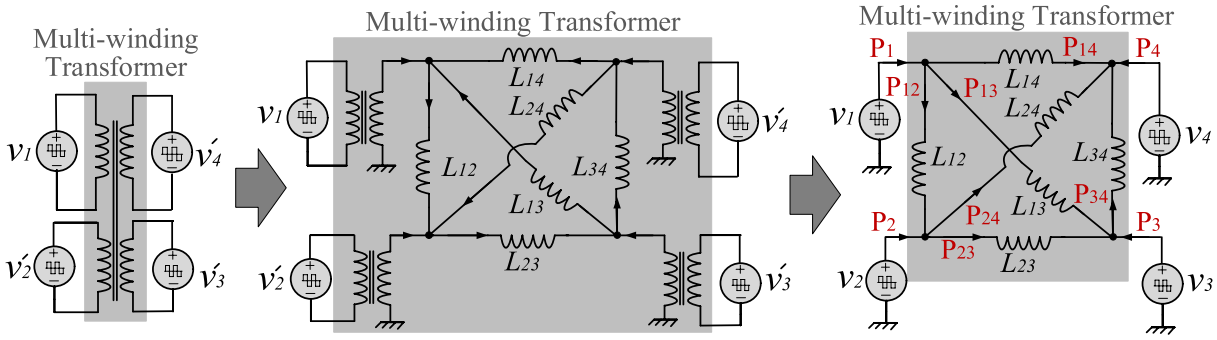

Fig. 3 Simplified model of the QAB converter by simplifying the multi-winding transformer using cantilever model

$$\begin{cases} P_1 + P_2 + P_3 + P_4 = 0 \\ P_1 = P_{12} + P_{13} + P_{14} \\ P_2 = P_{21} + P_{23} + P_{24} \\ P_3 = P_{31} + P_{32} + P_{34} \\ P_{ij} = -P_{ji} \quad \text{for} \quad i, j = 1, 2, 3, 4 \end{cases} \tag{1}$$

To control the amount and direction of power flow, the generated rectangular waveforms are phase-shifted from each other by controlled angles as presented in Fig. 4 for the waveforms of the PV and inverter ports. The angles are named as δ_{14} to control the power flows from PV to the inverter port, δ_{24} from wind turbine to the inverter port, δ_{13} PV to the battery, δ_{23} from wind turbine to the battery port and δ_{34} for the battery to the inverter port. The phase-shift δ_{ij} is positive when the voltage in port *i* lags the reference voltage in port *j* and negative when it leads the reference. The voltage of the inverter-linked winding is presented as v_4 does not have any duty cycle control and is selected as the reference due to its constant amplitude for convenience and the other generated waveforms have their duty cycles and phase-shift angles defined with respect to v_4. The power flows from port *i* to port *j* presented as P_{ij} when the waveform in port *i* is one of the PV, battery, and wind turbine ports are duty cycle controlled and *j* represents the port four where the waveform's duty cycle is one can be determined as

$$P_{ij} = \begin{cases} \frac{V_i V_j}{\omega L_{ij}} D\delta_{ij} & \left|\delta_{ij}\right| \le \frac{\pi}{2}(1-D) \\ \frac{V_i V_j}{\omega L_{ij}} \left[\delta_{ij}\left(1 - \delta_{ij}/\pi\right) - \text{Sign}(\delta_{ij})\frac{\pi}{4}(1-D)^2\right] & \frac{\pi}{2}(1-D) < \left|\delta_{ij}\right| \le \frac{\pi}{2} \end{cases} \tag{2}$$

where V_i is the dc voltage in port *i*, V_j the dc voltage in port *j*, ω the frequency of waveforms, L_{ij} the summation of leakage inductance in windings *i* and *j* and *D* duty cycle in the waveform of port *i* as presented in Fig. 4a. The amount of leakage inductance in each port depends on the maximum power generated or is planned to be transferred from each of the PV, battery or wind turbine ports to the inverter port. Therefore, the range of power in each port should be taken into account. On the other hand, the power flow between the two ports such as PV or wind turbine to the battery port where both waveforms have duty cycle controlled can be presented as

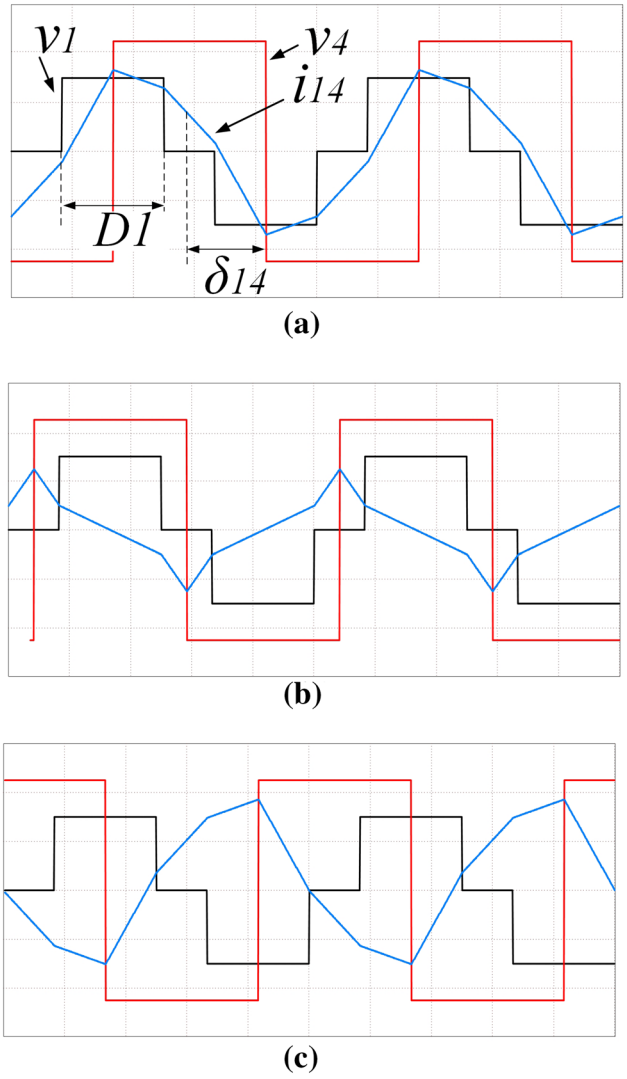

Fig. 4 The waveforms of voltage and current of port one and four in the transformer winding for three cases of **a** v1 is lagging v4, **b** v1 and v2 are in phase and **c** v1 is leading v2 where duty cycle of v1 (D1) and phase-shift angle are presented

windings are utilized as the main energy transfer elements [16, 42]. A dc conversion ratio can be defined between the converter ports as

$$d = \frac{V_i}{nV_j} \tag{4}$$

where $n = N_j/N_i$ is the transformer turns ratio, N_i and N_j are the numbers of turns of the transformer windings in ports *i* and *j*, respectively. Therefore, to analyze the four-port converter, the DAB converter topology should be considered as a basic step. In this topology, a full range of soft-switching operation is achievable when $d = 1$, which means an equal volt-second product of the voltage waveforms applied to the all transformer winding [24, 33]. In a lossless idealized circuit the maximum power flow between the ports can be determined from $\partial P_{ij}/\partial \delta_{ij} = 0$ which results in a maximum power at $\delta_{ij} = \pi/2$. However, the phase- shift angles greater than π/2 result in excessive reactive power, and therefore, the phase-shift is practically limited to less than π/2 [42].

3 Analysis of control system

The general structure of the hybrid renewable energy system and the control unit is presented in Fig. 5. The control unit is designed to operate in three different levels as presented in Fig. 6. The first level is a local controller, which controls the high-frequency switching devices of the converter based on the pulse width modulation (PWM) technique. The power flow between the converter ports is controlled at this stage, and the reaction time is normally in the range of microseconds to seconds depending on the range of switching frequency. In the second level, the energy management in the system is controlled by long-term data analysis and a processing unit. The result of this stage is normally applied in the form of setpoint signals to the first level controllers. The

$$P_{ij} = \begin{cases} \frac{V_i V_j D_i D_j}{\omega n L_{ij}(\max(D_i, D_j))}\delta_{ij} & \left|\delta_{ij}\right| \le \frac{\pi}{2}\left|D_i - D_j\right| \\ \frac{V_i V_j D_j}{\omega n L_{ij}}\left[\begin{array}{l} \mathrm{Sign}(\delta_{ij})\frac{\pi}{2}(D_i - D_j) + \delta_{ij} + \\ \frac{1}{D_j}\left[\mathrm{Sign}(\delta_{ij})\left(-\frac{\pi}{4}\right)(D_i^2 - D_j^2) + D_i\delta_{ij} - \mathrm{Sign}(\delta_{ij})\frac{\delta_{ij}^2}{\pi}\right] \end{array}\right] & \frac{\pi}{2}\left|(D_i - D_j)\right| < \left|\delta_{ij}\right| \le \frac{\pi}{2}(2 - D_i - D_j) \\ \frac{V_i V_j}{\omega n L_{ij}}\left[\delta_{ij}\left(1 - \frac{\delta_{ij}}{\pi}\right) - \mathrm{Sign}(\delta_{ij})\frac{\pi}{4}(1 - D_i)^2 - \mathrm{Sign}(\delta_{ij})(1 - D_j)^2\right] & \frac{\pi}{2}(2 - D_i - D_j) < \left|\delta_{ij}\right| \le \frac{\pi}{2} \end{cases} \tag{3}$$

where D_i and D_j are the duty ratio of v_i and v_j and $v_i/D_i = v_j/nD_j$ and $n = N_j/N_i$. The waveforms frequency is kept constant and the leakage inductance of the transformer

reaction time at this stage in the range of seconds to minutes. The long-term decision on the energy distribution in the system is normally taken in the third level

control and management unit. This stage is normally performed in the smart-grid control centers according to the long-term energy plans and historical data of the system, seasonal load profiles, and other factors. The reaction time at this stage is in the range of hours to days. The power flow equations in (2), (3) show that the duty cycle and phase-shift angle are the main elements that can be used as control variables. To discuss the control technique of the proposed converter, the simplified model of the phase-shift converter facilitates the analysis. The main issue related to the PV and wind turbine generator as renewable energy sources is their inherent intermittency and uncertainty. Therefore, the generated electrical energy is variable and there is not a constant operation point to set the converter ports. As a result, the converter operating point in the PV and wind turbine ports needs to be adjusted according to the maximum available energy at any time.

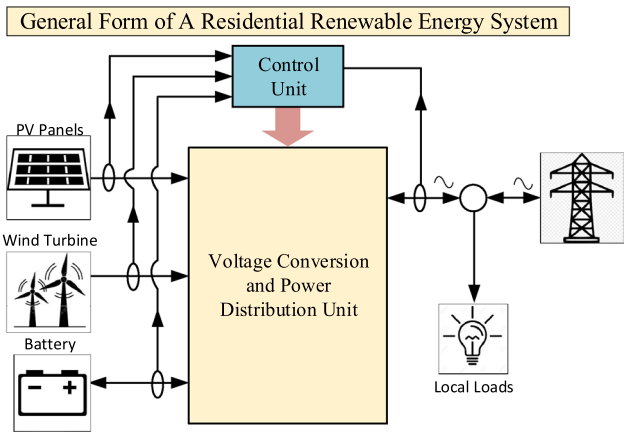

Fig. 5 General form of the proposed hybrid renewable energy system

The process is known as maximum power point tracking (MPPT) in the PV and wind turbine converter ports. On the other hand, the extracted electrical power from renewable energy sources should be continuously controlled and follows the load demand and the grid conditions and standards. In this paper, to realize the MPPT, the duty cycle of the switching devices in the H-bridge converters have been used as control variable. On the other hand, the phase-shift angle between the generated ac voltages at the converter ports is used to control the power flow between the converter ports. Therefore, the duty cycle control system should be designed to operate independently of the phase-shift controller. In theory, arbitrary power flow in the system can be realized by a unique set of phase shifts [16]. In the system proposed in this paper, there are multiple control objectives. The

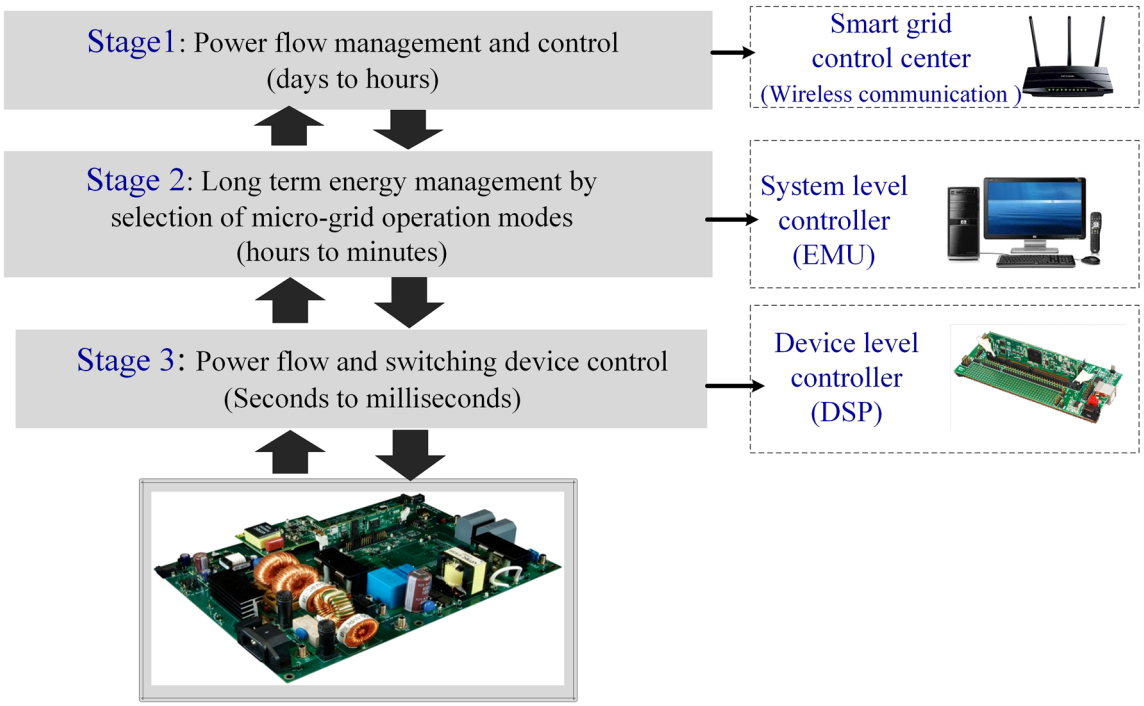

Fig. 6 Block diagram of the energy management system in brief

power flow control scheme aims to control the power flow between the ports while regulating the dc bus voltage of the port. Figure 7 illustrates the designed control system containing the control variables, reference signals provided by the master controller, and the control loops. The proportional-integral (PI) controllers have been used in the control loops to regulate the dc voltage and realize the MPPT operation. The PI controller transfer function is obtained as

$$G_C(S) = K_p + \frac{K_i}{S} \tag{5}$$

where K_p and K_i are the proportional and integral control coefficients and are set as 0.01 and 0.56, respectively. The power flow control in each converter port can be designed to regulate the voltage according to the provided reference signal. As voltage-type energy sources like wind turbine and PVs have a variable operating voltage, a power control strategy can be used as an equivalent of current control due to the slow change of the operating voltage of the source compared to the control bandwidth [16] and the dynamics of the power control loop is mainly determined by the port current.

Therefore, the dynamics of the voltage control loop can be ignored in the control design process, and it is regarded relatively constant value and as a gain in the control loop. Following this strategy, the extracted power from each of the renewable sources is controlled by using phase-shift angles (δ_{14}, δ_{24}, and δ_{34}) as the control variable. On the other hand, the DC bus voltage of the ports can be controlled by a proper selection of the duty cycles (D_1, D_2, and D_3) of the voltages at the PV-linked windings of the transformer. To reduce the control conflicts between the two variables (duty cycle and the phase shift), the dynamic response of the power flow control loop is designed to operate faster than the voltage control loop by designing proper controllers and adjusting K_p and K_i. On the other hand, to reduce the conflict between the control loops in different converter ports, the dynamic response of the power control loops has been designed to operate in different speeds according to the nature and characteristics of the connected source as presented in Fig. 8. As can be seen, the crossing frequency of wind turbine control loop is about 200 Hz as the slowest source and the battery as 30 kHz as the fastest source. The duty cycle control loops have crossing frequencies of less than 200 Hz for all three converter ports.

At the inverter side, a current control technique is used to force a unity power factor injected or received from the grid. Figure 9a shows the current control system designed for the grid-connected inverter. By using this

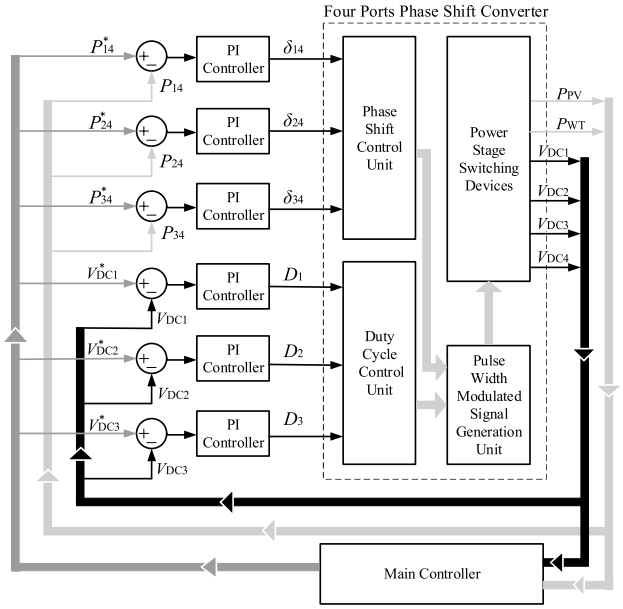

Fig. 7 The control system for multi-port converter in the proposed system

control system, the inverter output current compensates the leading or lagging current of the load (reactive element of the load power) to have a unity power factor at the grid-connected point. This is possible as referring to the current reference presented in Fig. 9b which shows that the grid current basically depends on the load and inverter currents ($i_g = i_o - i_L$). The energy management in the system uses the recorded data from previous operation times, the real-time value of the system parameters including voltage and current and energy cost as the main factors in determining the best operation scenario for the system. So the operation scenarios and power flow directions in each scenario are selected to satisfy the objective function in the best way. Details of the energy management is out of the scope of this paper and will be covered in future reports.

4 Numerical simulations

The proposed system has been simulated using PSIM and the proposed control technique is implemented to control the power flow between the ports. The system can operate in different operation modes and the power can flow between the converter ports in different ways. A proper selection of the operation modes during a time frame is known as energy management scenario and different energy management scenarios considering various effective factors have been presented in the literature [17, 25]. This paper is mainly focused on the operation principle

and control technique of the proposed system and energy management discussions is out of the scope of this paper and will be presented in detail in future publications. To provide a better understanding of the converter operation, some of the simulated waveforms of voltages and currents in the converter and grid-connected inverter have been presented and studied in this section.

The system parameters that have been selected in the numerical simulation are illustrated in Table1. The waveforms of the voltage and current in the windings of transformer for the PV, wind turbine and inverter ports have been presented in Fig. 10 for two different cases of the phase-shift angles and duty cycles. The power is transferred from the PV and wind turbine ports to the inverter port as the voltage at the PV and wind turbine ports is leading to the inverter port in both cases. The currents in the windings of the transformer have also been presented. The battery port is deactivated in the both cases and only three converter ports are active. As can be seen, the high-frequency voltage generated in the inverter port is not duty cycle controlled in both cases; however, the duty cycle of the voltage of at the wind turbine port is controlled in the case (b) to adjusting the dc bus voltage and compensate for slight increase in the wind turbine output voltage.

Figure 11 shows the inverter output waveform. The main objective for the inverter is to supply the load and possibly the grid from renewable energy sources or transfer the energy in reverse direction from the grid to the battery to charge the battery when is required. However, any energy transfer to/from the grid should be under the unity power factor as the main condition for the grid-connected residential renewable energy systems. Therefore, the inverter output is controlled to provide the required output current with a proper phase-shift angle to satisfy the mandatory conditions. This was already discussed in the controller design section. Figure 11a shows the output voltage and current of the inverter before filtering for the unity power factor. Figure 11b presents a case that the inverter is supplying the load and the grid. As the load current is slightly lagging the voltage, the inverter output is compensating the difference to force the grid current toward a unity power factor as $i_g = i_o - i_L$ considering i_o as the inverter output current, i_L as the load current and i_g as the injected current into the utility grid. In the second case as presented in Fig. 11c, the power flows in the opposite direction from the grid to the load and inverter (charging

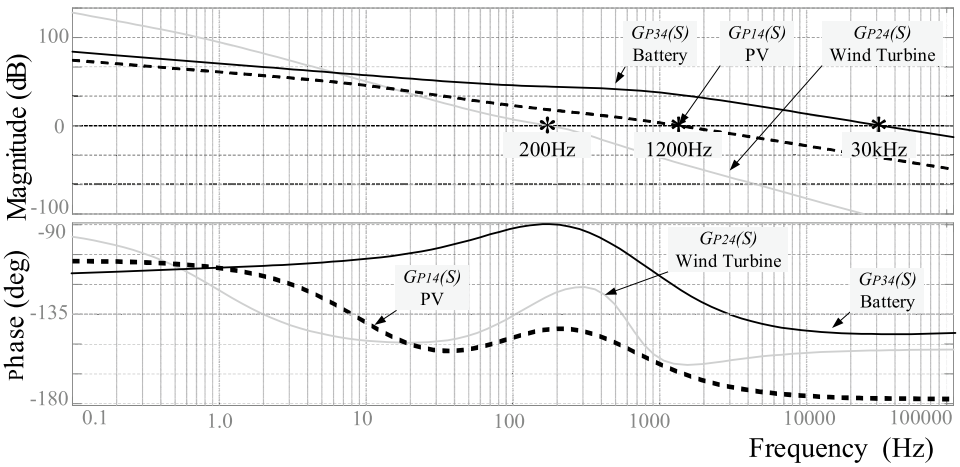

Fig. 8 The magnitude and phase Bode diagrams of the power control closed-loop transfer functions

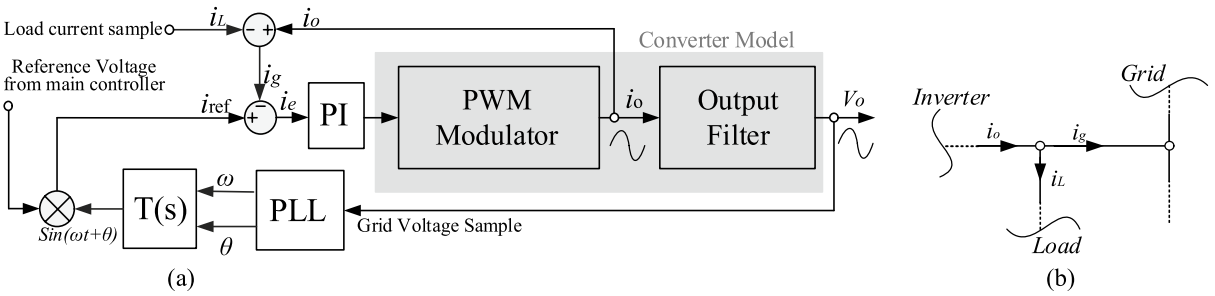

Fig. 9 **a** The control system for the grid-connected inverter and **b** current direction reference in the inverter output

the battery). In this case, the inverter is operating as a rectifier in the reverse direction and the received current adjusted properly to compensate for the slight phase shift in the load current due to the inductive load effect.

To study the dynamic response of the power flow control, two different cases of power flow control have been presented in Fig. 12. As can be seen, in the first case, the response of the system to a step changes in the load while the output power extracted from PV and the wind turbine is almost constant. The difference between the load demand and renewable power is compensated by the battery. However, it can also be supplied by the utility grid depending on the availability of the battery energy and the cost of the grid energy compared to the battery at the presented time. The load demand variation is simulated by adding/removing a resistor in parallel with the output filter capacitor. In the second case, the load is supplied by the battery, grid and wind turbine. When the load demand is increased, the demand is covered by the grid at the first stage. However, after a transient time the battery port is activated to undertake the demand–supply, and therefore, the grid power is reduced to the previous value. The command for changing operation conditions is normally provided by the main control energy management section and the detail of energy management will be provided in future publications.

Table 1 System parameters for numerical simulations

Parameters	Values
Leakage inductance of transformer windings	L1 = 0.012 mH, L2 = 0.01 mH, L3 = 0.008 mH, L4 = 0.02 mH
Number of turns of each winding of the transformer	$N_1 = 7$, $N_2 = 6$, $N_3 = 5$, $N_4 = 18$
Magnetizing inductance Lm	$L_m = 1.12$ mH
Rated power in each input of the converter	$P_{PV} = 1200$ W, $P_{BT} = 600$ W, $P_{WT} = 800$ W
PV characteristics (totally six panels connected in two paralleled branches)	Each panel: Vo = 35 V, $I_{max} = 6$ A , $P_{max} = 200$ W
Switching frequency of the multi-port converter	$f_{sc} = 15$ kHz
DC bus voltage	V1 = 110 V, V2 = 100 V, V3 = 80 V, V4 = 300 V
Switching frequency of inverter	$f_{si} = 10$ kHz
Utility grid parameters	f=50 Hz, V(rms)=150 V
Wind turbine characteristics	V = 100 V dc, P = 800 W , $I_{max} = 9$ A

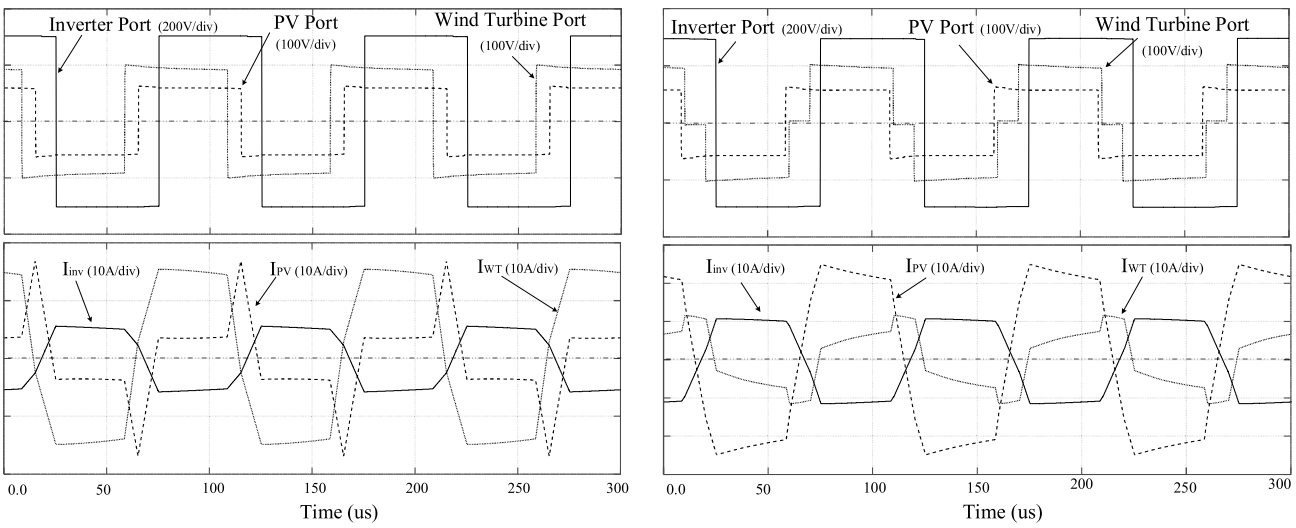

Fig. 10 The waveforms of the voltage and current in the multi-winding transformer **a** where duty cycle in both PV and wind turbine ports is not controlled and, **b** the duty cycle in the wind turbine port is controlled

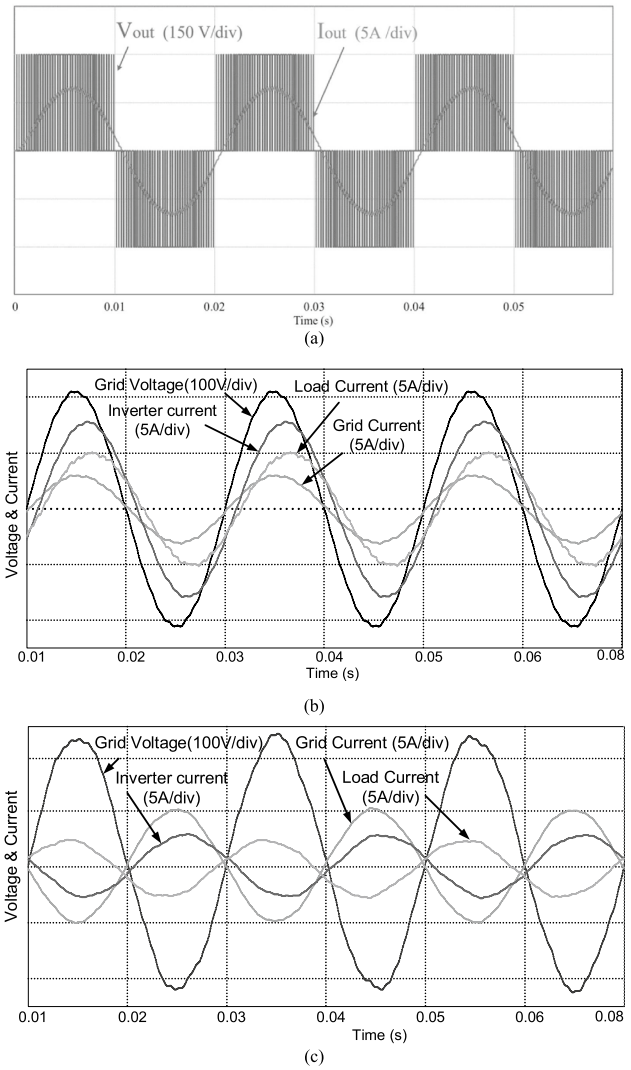

Fig. 11 **a** the inverter output voltage before filtering and the output current, **b** when power is transferred from the inverter to the grid and the load and, **c** when inverter is operating as rectifier and power is transferred in opposite direction from grid to the load and battery reduced back to the previous value

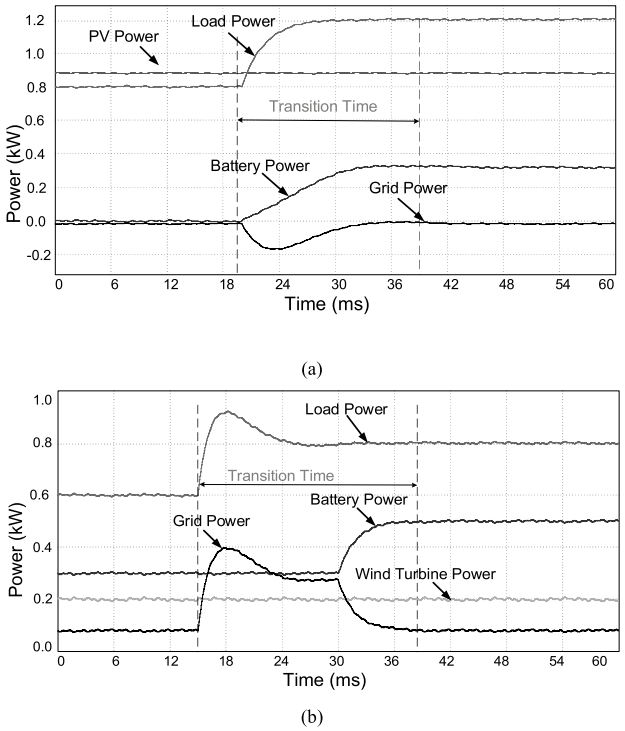

Fig. 12 Step response in the load demand and operation of the proposed system in compensation of load demand **a** when the load demand is compensated by the battery during the transition time, and **b** when the load demand is compensated by the utility grid during the transition time

5 Experimental tests

To validate the designed converter, a prototype of the proposed converter was developed in the lab as can be seen in Fig. 13. Two DSP controllers (C2000/ TMS320F28335) made by Texas Instruments are used as local controllers to control the multi-port phase-shift dc–dc converter and the single-phase inverter. A Laptop (Asus, FK003QM, CPU: Intel-core i7, 2.6 GHz, 12 GB RAM) has been used as a master or global controller for energy management and data record and analysis. The Hall effect voltage (LV 25-P) and current (LTSR25-NP) sensors are used to measure the voltage and currents. The output voltage and currents of the single-phase inverter in different active and reactive power conditions is presented in the following figures.

As can be seen in Fig. 14a, the reactive power has been changed from 1.5 to 2.25 kVAR and is of inductive type. However, the active power remained almost constant during the step change. The control system presented an acceptable performance to follow the applied step change. In Fig. 14b, the reactive power injected to the utility grid by the inverter has been changed from inductive (2.55 kVAR) to the

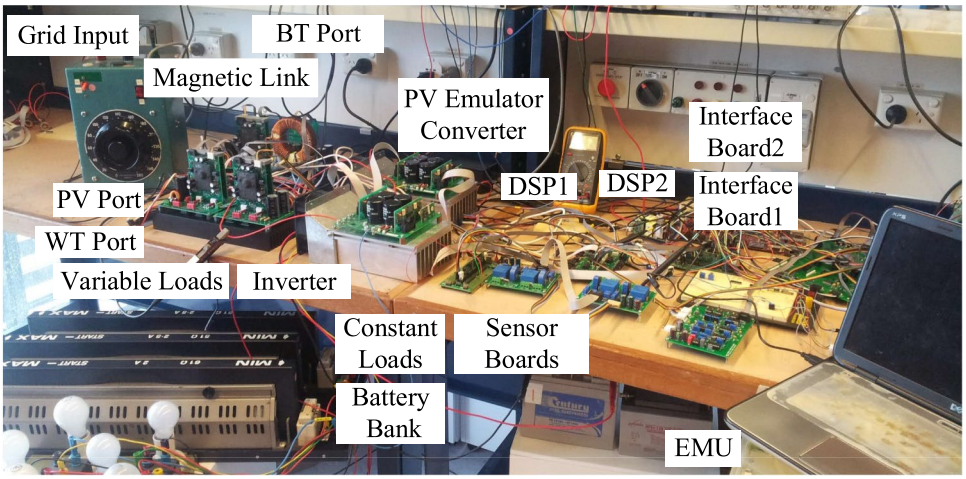

Fig. 13 The experimentally developed multi-port converter

capacitive (2.54 kVAR) with an almost constant active power (≈0.12 kW). This shows the ability of the proposed converter in reactive power compensation and improvement of the utility grid parameters such as voltage and frequency in a limited range. To show the bidirectional power from the to/from the utility grid, the power flow from inverter to the grid has been changed sharply changed to an opposite direction from the grid to the converter to charge the battery as illustrated in Fig. 14c. In this case, the inverter is operated in the reverse direction as a rectifier and the energy transferred from the grid to the battery. This shows the ability of the proposed converter to be used as a virtual power plant and operate as an assistant to the utility grid and also provides benefits for the consumer. As can be seen the inverter is supplying 1.83 kW to the load and utility grid and then the active power is changed to the 1.73 kW in the reverse direction to charge the battery. The experimental test results show that the proposed system can be used successfully not only to supply the load but also to improve the utility grid performance.

6 Conclusions

A multi-port converter topology for integrating a PV system, a wind turbine generator and a battery is presented in the paper to supply a grid-connected domestic load. The operation principle and control technique of the proposed system shown in detail. To validate the system topology and control technique, numerical simulations have been performed using PSIM software. The waveforms of the voltage and currents of the multi-port converter and inverter and the dynamic response of the system under a step-change in the load have been presented and analyzed.

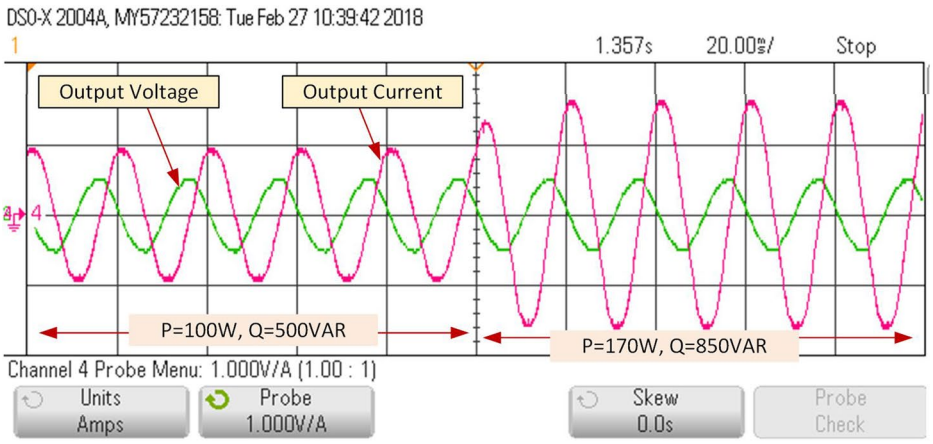

(a)

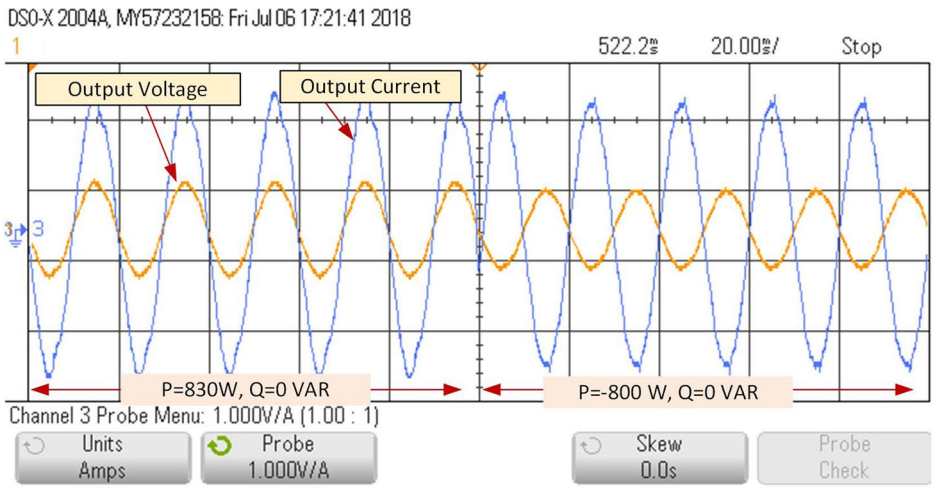

(b)

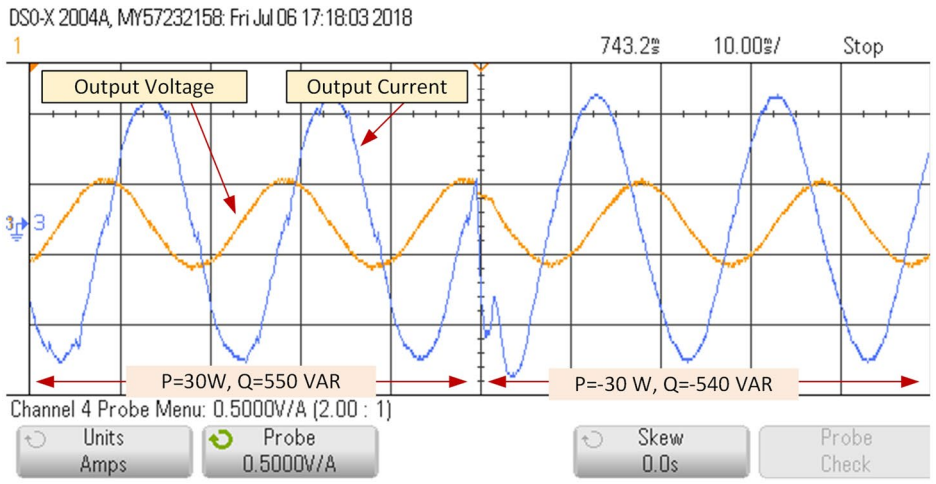

(c)

Fig. 14 The experimental test results for power flow control, **a** the reactive power has been changed from 1.5 kVAR to 2.25 kVAR and is of inductive type, **b** the reactive power injected to the utility grid by the inverter has been changed from inductive (2.55 kVAR) to the capacitive (2.54 kVAR) and, **c** the inverter is supplying 1.83 kW to the load and utility grid and then the active power is changed to the 1.73 kW in reverse direction to charge the battery

Compliance with ethical standards

Conflict of interest The authors declare that they have no conflict of interest.

References

1. Tao H, Duarte JL, Hendrix MAM (2008) Three-port triple-half-bridge bidirectional converter with zero-voltage switching. IEEE Trans Power Electro 23(2):782–792. https://doi.org/10.1109/TPEL.2007.915023
2. Jafari M, Malekjamshidi Z, Zhu J (2017) Design, analysis and control of a magnetically-coupled multi-port multi-operation-mode residential micro-grid. In: 2017 20th international conference on electrical machines and systems (ICEMS), Sydney, NSW, pp. 1–6. DOI: https://doi.org/10.1109/ICEMS.2017.8056449
3. Zhao C, Round S, Kolar JW (2005) Buck and boost start-up operation of a three-port power supply for hybrid vehicle applications. Proceedings IEEE Power Electronics Specialists Conference (PESC'05), Recife, Brazil, Jun. 2005, pp 1851–1857. https://doi.org/10.1109/PESC.2005.1581883
4. Malekjamshidi Z, Jafari M, Imanieh M (2011) Implementation of a full bridge series-parallel resonant DC-DC converter using ANN and SSM controllers. Proceedings of the 2011 IEEE National Aerospace and Electronics Conference (NAECON), Dayton, OH, pp 203–210. DOI: https://doi.org/10.1109/NAECON.2011.6183102
5. Jafari M, Malekjamshidi Z, Jian Guo Zhu (2012) Design, simulation and implementation of an intelligent MPPT using a ZVCS resonant DCDC converter. In: 2012 IEEE international conference on Power and Energy (PECon), Kota Kinabalu, pp 280–285. DOI: https://doi.org/10.1109/PECon.2012.6450222
6. Jafari M, Malekjamshidi Z, Islam MR, Zhu J (2014) Comparison of singular and modular structures of multi-port converters for residential applications in smart grids. In 2014 IEEE Innovative Smart Grid Technologies-Asia (ISGT ASIA), Kuala Lumpur, pp 606-611, doi: 10.1109/ISGT-Asia.2014.6873861
7. Jafari M, Malekjamshidi Z (2011) "Design, simulation and implementation of an adaptive controller on base of artificial neural networks for a resonant DC-DC converter, In: 2011 IEEE ninth international conference on power electronics and drive systems, Singapore, pp 1043–1046, doi: https://doi.org/10.1109/PEDS.2011.6147388
8. Malekjamshidi Z, Jafari M, Islam MR, Zhu, J (2014) "A comparative study on characteristics of major topologies of voltage source multilevel inverters. In: 2014 IEEE Innovative Smart Grid Technologies-Asia (ISGT ASIA), Kuala Lumpur, pp 612–617. DOI: 10.1109/ISGT-Asia.2014.6873862
9. Alajmi BN, Marei MI, abdelsalam IA (2020) A multi-port DC/DC converter based on two-quadrant inverter topology for PV systems. IEEE Trans on Power Electron. https://doi.org/10.1109/TPEL.2020.3002504
10. Liu YC, Chen YM (2007) A systematic approach to synthesizing multiple-input dc–dc converter. IEEE Trans Power Electron 24(1):116–127. https://doi.org/10.1109/TPEL.2008.2009170
11. Benavides ND, Chapman PL (2005) Power budgeting of a multiple-input buck-boost converter. IEEE Trans Power Electron 20(6):1303–1309
12. Dobbs BG, Chapman PL (2003) A multiple-input DC-DC converter topology. IEEE Power Electron Lett 1(1):6–9
13. Jafari M, Hunter G, Zhu JG, (2012) A new topology of multi-input multi-output buck-boost DC-DC converter for microgrid applications. In: 2012 IEEE International Conference on Power and Energy (PECon), Kota Kinabalu, pp. 286–291. DOI: https://doi.org/10.1109/PECon.2012.6450223
14. Duarte JL, Hendrix M, Simões MG (2007) Three-port bidirectional converter for hybrid fuel cell systems. IEEE Trans Power Electron 22:480–487. https://doi.org/10.1109/TPEL.2006.889928
15. Tao H, Kotsopoulos A, Duarte J, Hendrix M (2006) Family of multi-port bidirectional DC–DC converters. IEE Proc Electr Power Appl 153:451. https://doi.org/10.1049/ip-epa:20050362
16. Tao H (2008) Integration of sustainable energy sources through power electronic converters in small distributed electricity generation systems. Phd thesis, Eindhoven: Technische Universiteit Eindhoven
17. Jafari M (2019) Malekjamshidi, Z & Zhu, J 2019, "A magnetically coupled multi-port, multi-operation-mode micro-grid with a predictive dynamic programming-based energy management for residential applications." Int J Electr Power Energy Syst 104(January):784–796. https://doi.org/10.1016/j.ijepes.2018.07.040
18. Jafari M, Malekjamshidi Z, Islam MR, Zhu J (2015) Modeling of magnetic flux in multi-winding toroidal core high frequency transformers using 3D reluctance network model. In: 2015 IEEE 11th International Conference on Power Electronics and Drive Systems, Sydney, NSW, pp 413–418. DOI: https://doi.org/10.1109/PEDS.2015.7203546
19. Jafari M, Malekjamshidi Z, Zhu J, Khooban M (2018) Novel predictive fuzzy logic-based energy management system for grid-connected and off-grid operation of residential smart micro-grids. IEEE J Emerg Sel Top Power Electron. https://doi.org/10.1109/JESTPE.2018.2882509
20. Tao H, Kotsopoulos A, Duarte JL, Hendrix MAM (2008) Transformer-coupled Multiport ZVS bidirectional DC–DC converter with wide input range. IEEE Trans Power Electron 23(2):771–781
21. Jafari M, Malekjamshidi Z, Zhu J (2019a) Copper Loss Analysis of a Multiwinding High-Frequency Transformer for a Magnetically-Coupled Residential Microgrid. IEEE Trans Ind Appl 55(1):283–297. https://doi.org/10.1109/TIA.2018.2864170
22. Barrios EL, Ursúa A, Marroyo L, Sanchis P (2015) Analytical design methodology for Litz-Wired high-frequency power transformers. IEEE Trans Ind Electron 62(4):2103–2113
23. Jafari M, Malekjamshidi Z, Lei G, Wang T, Platt G, Zhu J (2017) Design and implementation of an amorphous high-frequency transformer coupling multiple converters in a smart microgrid. IEEE Trans Ind Electron 64(2):1028–1037. https://doi.org/10.1109/TIE.2016.2583401
24. Jafari M, Malekjamshidi Z, Zhu J (2019b) Design and development of a multi-winding high-frequency magnetic link for grid integration of residential renewable energy systems. Appl Energy 242:1209–1225. https://doi.org/10.1016/j.apenergy.2019.03.124
25. Chen Y-M, Liu Y-C, Wu F-Y (2002) Multi-input DC/DC converter based on the multiwinding transformer for renewable energy applications. IEEE Trans Ind Appl 38:1096–1104. https://doi.org/10.1109/tia.2002.800776
26. Michon MM, Duarte JL, Hendrix M, Simoes MG, (2004) A three-port bi-directional converter for hybrid fuel cell systems. IEEE Power Electronics Specialists Conference (PESC'04), Aachen, Germany, Jun. 2004, pp 4736–4742. DOI: https://doi.org/10.1109/PESC.2004.1354836
27. Zhao C, Kolar JW (2004) A novel three-phase three-port UPS employing a single high-frequency isolation transformer. IEEE Power Electronics Specialists Conference (PESC'04), Aachen, Germany, Jun. 2004, pp 4135–4141. DOI: https://doi.org/10.1109/PESC.2004.1354730
28. Jafari M, Malekjamshidi Z, Lu DD, Zhu J (2019) Development of a fuzzy-logic-based energy management system for a multiport

multioperation mode residential smart microgrid. IEEE Trans Power Electron 34(4):3283–3301. https://doi.org/10.1109/TPEL.2018.2850852
29. Jafari M, Platt G, Malekjamshidi Z, Zhu JG (2015) Technical issues of sizing Lead-Acid batteries for application in residential renewable energy systems. In: 2015 4th International Conference on Electric Power and Energy Conversion Systems (EPECS), Sharjah, pp 1–6. DOI: https://doi.org/10.1109/EPECS.2015.7368533
30. Liu D, Li H (2006) A ZVS bi-directional DC-DC converter for multiple energy storage elements. IEEE Trans Power Electron 21(5):1513–1517. https://doi.org/10.1109/TPEL.2006.882450
31. Jafari M, Malekjamshidi Z, Li L, Zhu JG (2013) Performance analysis of full bridge, boost half bridge and half bridge topologies for application in phase shift converters. In: 2013 International Conference on Electrical Machines and Systems (ICEMS), Busan, pp 1589–1595. DOI: https://doi.org/10.1109/ICEMS.2013.6713326
32. Jafari M, Malekjamshidi Z, Platt G, Zhu JG, Dorrell DG (2015) A multi-port converter based renewable energy system for residential consumers of smart grid. IECON 2015-41st Annual Conference of the IEEE Industrial Electronics Society, Yokohama, pp 005168–005173. DOI: https://doi.org/10.1109/IECON.2015.7392911
33. Shi Y, Li R, Xue Y, Li H (2016) High-frequency-link-based grid-tied PV system with small DC-link capacitor and low-frequency ripple-free maximum power point tracking. IEEE Trans Power Electron 31(1):328–339. https://doi.org/10.1109/TPEL.2015.2411858
34. Chen G, Xu D, Wang Y, Lee Y (2001) A new family of soft-switching phase-shift idirectional DC–DC converters. IEEE Power Electronics Specialists Conference (PESC'01), Jun. 2001, pp 859–865. DOI: https://doi.org/10.1109/PESC.2001.954227
35. Jafari M, Islam MR, Malekjamshidi Z, Zhu J (2015) Modeling of multi-winding high-frequency transformers as a common magnetic-link in smart micro-grids. In: 2015 International Conference on Electrical & Electronic Engineering (ICEEE), Rajshahi, pp 249–252. DOI: https://doi.org/10.1109/CEEE.2015.7428269
36. Kheraluwala MH, Gascoigne RW, Divan DM, Baumann ED (1992) Performance characterization of a high-power dual active bridge DC-to-DC converter. IEEE Trans Ind Appl 28(6):1294–1301
37. Vangen K, Melaa T, Bergsmark S, Nilsen R, Efficient high-frequency soft-switched power converter with signal processor control. IEEE Telecommunications Energy Conference (INTELEC'91), Nov. 1991, pp 631–639. DOI: https://doi.org/10.1109/INTLEC.1991.172460
38. Vangen K, Melaa T, Adnanes AK (1992) Soft-switched high-frequency, high power DC/AC converter with IGBT, IEEE Power Electronics Specialists Conference (PESC'92), Jun. 1992, pp 26–33. DOI: https://doi.org/10.1109/PECon.2012.6450223
39. Vangen K, Melaa T, Adnanes AK, Kristiansen PE, Dual active bridge converter with large soft-switching range, Fifth European Conference on Power Electronics and Applications (EPE'93), Sep. 1993, pp 328–333
40. Zhang JM, Xu DM, Qian Z (2001) "An improved dual active bridge DC/DC converter. IEEE Power Electronics Specialists Conference (PESC'01), Vancouver, BC, Canada, Jun. 2001, pp 232–236. DOI: https://doi.org/10.1109/PESC.2001.954025
41. Zhang J, Zhang F, Xie X, Jiao D, Qian Z (2004) A novel ZVS DC/DC converter for high power applications. IEEE Trans Power Electron 19(2):420–429
42. Jafari M, Malekjamshidi Z, Zhu JG (2015) Analysis of operation modes and limitations of dual active bridge phase shift converter. In: 2015 IEEE 11th International Conference on Power Electronics and Drive Systems, Sydney, NSW, 2015, pp 393–398. DOI: https://doi.org/10.1109/PEDS.2015.7203545